VTT Technical Research Centre of Finland

Small- to medium-scale deep syngas purification

Frilund, Christian; Tuomi, Sanna; Kurkela, Esa; Simell, Pekka

Published in:
Biomass and Bioenergy

DOI:
10.1016/j.biombioe.2021.106031

Published: 01/05/2021

Document Version
Publisher's final version

License
CC BY

Biomass and Bioenergy 148 (2021) 106031

Contents lists available at ScienceDirect

Biomass and Bioenergy

journal homepage: http://www.elsevier.com/locate/biombioe

Small- to medium-scale deep syngas purification: Biomass-to-liquids multi-contaminant removal demonstration

Christian Frilund *, Sanna Tuomi, Esa Kurkela, Pekka Simell

VTT Technical Research Centre of Finland Ltd, P.O. Box 1000, FI-02044 VTT, Finland

ARTICLE INFO

Keywords:
Syngas cleaning
Ultracleaning
Adsorption
Biomass-to-liquids
Gasification
Process validation
Hydrogen sulfide
Water scrubbing

ABSTRACT

The complete and economic removal of harmful components from biomass gasification-based syngas is a major challenge. A final gas cleaning concept for syngas purification to catalytic synthesis quality was developed as an alternative to organic-solvent scrubbing technologies. The motivation is to present smaller-scale BTL processes with a potentially lower-capex gas cleaning solution. The purpose of this study was to realize and validate the final gas cleaning concept in a real syngas environment and to study longer-term performance of deep gas cleaning. Two successful PDU-scale campaigns in complete biomass-to-liquids production chain were performed. A total on-stream time of 163 h was realized in syngas generated from residual woody- and agro-biomasses, with coupled gas feeding to Fischer-Tropsch synthesis. For S-species removal the final gas cleaning featured a novel hybrid of activated carbon- and ZnO-based bed materials. NH_3 and partial CO_2 removal was achieved by pressurized water scrubbing. The campaigns employed extensive continuous and non-continuous analysis techniques for the study of syngas impurities such as H_2S, COS, NH_3, HCN, HCl, benzene and tar. The final gas cleaning process demonstrated flexible deep removal of syngas contaminants of all tested biomass origins, thus achieving similar or better purification levels as conventional wet-scrubbing technologies. The cleaned gas was therefore suitable for catalytic synthesis purposes, demonstrating the technical feasibility of the new final cleaning process in conjunction with optimized hot gas cleaning.

1. Introduction

BTL-processes (biomass-to-liquids) are one of the most researched topics for the production of carbon-neutral synthetic transportation fuels or chemicals. Biomass as well as other carbonaceous feedstocks can be converted via thermochemical gasification route to synthesis gas and finally to liquid products [1]. However, several techno-economic studies [2–5] have concluded that gasification based BTL concepts require very large scales in order to achieve positive economics. Consequently, small-to medium scale (<200 MW biomass input) facilities require reconceptualization of the design to be feasible. The control and management of syngas impurities has always been one of the biggest bottlenecks to commercial deployment of BTL processes. In the area of "final gas cleaning" i.e deep gas cleaning to meet strict end-use requirements for synthesis, most BTL concepts utilize existing technologies that originate from fossil fuel conversion. Significant cost saving benefits could be achieved by replacing these with optimized cleaning processes at relatively small biomass conversion plants.

The aim of the research was to develop a simplified "lower-capex" final gas cleaning process for trace impurities removal based on a hybrid of adsorption materials. The concept was constructed and evaluated at process development unit (PDU) -scale in a complete biomass-to-liquids process configuration. The intention of the experimental campaigns was to gain new knowledge of the challenges and opportunities of deep gas cleaning in a real syngas environment.

2. Final gas cleaning

Comprehensive bio-syngas clean-up presents several challenges. It requires treating a wide range of contaminants present in various concentrations. Cleaning is further complicated by the inherent inhomogeneity of biomass [6]. These impurities can include particulates, organic tars, sulfur species (mainly hydrogen sulfide (H_2S), but also carbonyl sulfide (COS), carbon disulfide (CS_2) and organic sulfur such as thiophene), halogens (mainly as chlorine), nitrogen-species (mostly ammonia (NH_3), but also hydrogen cyanide (HCN)) and alkali metals (mainly Na, K) [7]. Table 1 presents estimates of impurities content after a hot gas cleaning section (hot filtration and tar reforming), adapted from previous studies of similar gasification facilities [8,9]. Also

* Corresponding author.
E-mail address: christian.frilund@vtt.fi (C. Frilund).

https://doi.org/10.1016/j.biombioe.2021.106031
Received 6 November 2020; Received in revised form 19 February 2021; Accepted 28 February 2021
Available online 18 March 2021

Abbreviations

AR	Adsorption reactor
AWC	Acid wash condenser
BFB	Bubbling fluidized bed (gasifier)
BT	Buffer Tank
BTL	Biomass-to-Liquids
BTX	Benzene, Toluene, Xylene
CGB	Cold Guard Bed
CP	Compressor
CR	Catalytic reformer
FID	Flame ionization detector
FWR	Forest wood residues
HF	Hot filtration
LoD	Limit of detection
n.a	Not analysed
n.d	Not detected
OGP	Off-gas purge
PDU	Process development unit
PWS AC	Pressurized Water Scrubber: Absorption column
PWS DC	Pressurized Water Scrubber: Desorption column
RH	Relative humidity
RME	Rapeseed Oil Methyl Ester
RR	Removal rate
WGB	Warm Guard Bed

Table 1
Estimates of steam fluidized bed gasification gas impurities concentrations after hot gas cleaning section, and gas purification requirements for Fischer-Tropsch application.

Impurity ($cm^3\ m^{-3}$)	Fluidized-bed gasification (steam)		Purity requirement (FT catalyst)	
	Woody-residues	Agro-residues	Leibold et al. (SASOL) [10]	Boerrigter et al. [11]
H_2S	20–200	40–400	<0.01	<1
COS	2–20	1–40		
HCN	0.5–5	1–10	<0.02	<1
NH_3	50–500	100–1000		
Halides	<2	<5	<0.01	<0.01
Alkalis	<1	<1	<0.01	<0.01
Tars	<1000	<4000	Below dew point	Below dew point

included are literature estimates of the Fischer-Tropsch synthesis catalyst impurities tolerance.

For synthesis catalysts, the catalyst poisoning effect of sulfur species is perhaps best known, and it is reported that H_2S adsorbs more rapidly to the surfaces and forms metal sulfides than COS and organic sulfurs. For Co-based FT catalysts an ex-situ catalyst poisoning study [12] showed that a 2000 $cm^3\ m^{-3}$ sulfur loading caused almost full deactivation. However, the catalyst impurity tolerance is also an economic parameter where the investment in final gas cleaning versus catalyst lifetime need to be weighed [13].

Syngas cleaning can generally be divided into cold (where water vapour condensation occurs), medium (100–300 °C) and hot processes (>300 °C) [14]. Hot processes generally involve catalytic routes for converting contaminants while cold processes often use techniques for separating species from the gas. The main drawbacks of cold gas cleaning methods in the BTL context is mainly 1) Thermal efficiency penalty due to syngas cooling 2) Cost incurred for treatment or disposal of contaminant streams, which in wet processes are solvent effluents and in dry processes spent adsorbents/catalysts [6]. Cold gas cleanup methods are often considered more proven technology, thus the final gas cleaning in the BTL concept of this work is based on cold processes.

High acid-gas content streams are conventionally purified using organic solvent-based wet scrubbing technologies, either by physical absorption, such as Rectisol and Selexol processes, or chemical absorption, which are amine-based processes [15–17]. The acid-gas scrubbing processes can however represent up to 20% (due to the process complexity, extreme process conditions and required gas treating units [17]) of the initial capital investments if applied to a medium-scale BTL concept, and consequently simpler alternatives to solvent-scrubbing methods are pursued [18].

Beyond conventional solvent-based solutions, several syngas purification processes for BTL demonstrations have been realized in research in the past years. The Bioliq® demonstration plant from Karlsruhe Institute of Technology (KIT) utilizes hot syngas cleaning concept where acid gases by alkali adsorbents and N-species removal by catalytic decomposition [19]. The GoBiGas demonstration plant employed an RME scrubber step followed by several steam regenerated fixed activated carbon beds for removal of mainly BTX compounds, but also H_2S and other trace contaminants. COS hydrolysis was performed separately [20,21]. In a similar manner Güssing biomass DFB gasification demonstration plant the syngas cleaning for Fischer-Tropsch application was achieved by an atmospheric RME scrubbing step, followed by activated carbons. Pressurized fixed bed reactors involving Ni-based HDS catalyst (organic sulfur removal), ZnO and CuO adsorbents and Na-based adsorbents for HCl removal were utilized [22–24]. The varying methods by which purified syngas is achieved highlights that each solution is tailored according to the specific gas impurity profile and content.

2.1. Final gas cleaning process concept

In this work we examine an integrated BTL concept, which co-produces FT syncrude and heat. Here primary tar control is carried out in the gasification and hot filtration units and finally by a simple, robust and highly effective catalytic reformer, as illustrated in the simplified BTL concept block diagram in Fig. 1 [9].

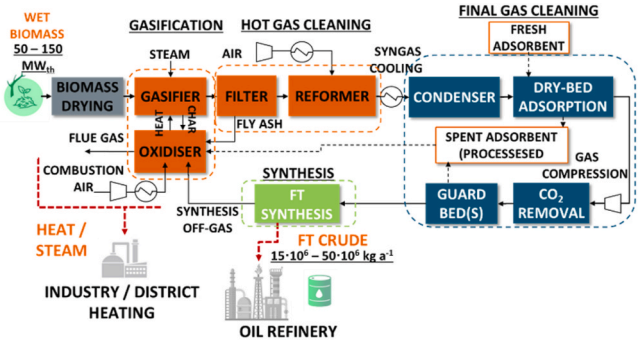

Fig. 1. Schematic block of BTL concept co-producing FT syncrude and heat.

Table 2
Final gas cleaning concept unit operations and function.

Unit	Function
Condenser	Condensing of water vapour, and acid injection for NH_3 removal
Adsorption I	Dry-bed adsorptive bulk H_2S removal (AC- or ZnO-based) and removal of trace contaminants such as benzene, tars, halogens, alkali (AC-based)
Guard Bed I	Dry-bed heated (200 °C) unit for catalytic conversions: •COS/HCN hydrolysis •Optional Deoxygenation
Guard Bed II (Water Scrubber)	Optional dry-bed activated carbon-based final polishing step (Optional pressurized water scrubber for partial CO_2 removal)

The multifunctional hot gas filtration unit not only removes dust particles, condenses alkali- and heavy metals, but removes parts of the tars as well [25]. The comprehensive hot gas cleaning section reduces the complexity of the final gas cleaning process by removing the need for a separate tar scrubbing steps. Calcium-containing gasifier bed materials such as limestone or dolomite act as tar decomposing catalysts and in-situ adsorbents for H_2S removal, thus also simplifying downstream cleaning [26,27]. Furthermore, Ni-based reforming catalysts have shown to promote NH_3 decomposition to N_2 and H_2 [28–30].

Based on the estimated gas purity requirements for synthesis, a final gas cleaning process was designed that was optimized for the impurity target levels presented in Table 1, while retaining flexibility for variations in their concentration. The design is based on low-cost adsorption and organic solvent-free scrubbing removal methods that are simple and proven unit operations. Table 2 outlines the envisioned major units of the process and their primary function.

The process involves up to five steps, depending on the desired gas purity requirements, and are operated at low-to medium temperatures. Cold gas cleaning solutions for NH_3 typically involve absorption. NH_3 readily protonates in water, but removal is further improved in an acidic solution, which is why an acid washing step is included in the concept [6].

Activated carbon (AC) is a high surface-area potentially low cost (<1 \$ kg^{-1}) adsorbent material that can be tailored by impregnation or surface modification to facilitate the removal of several types of impurities present in syngas [31,32]. It can remove both inorganic and organic compounds at low temperatures, whereas ZnO is suitable for inorganic trace impurity removal at medium temperatures [11]. In the BTL concept H_2S is removed using activated carbons by physical adsorption or by a more effective selective oxidation route at low temperatures according to Reaction 1 [33,34].

$$H_2S + \frac{1}{2}O_2 \rightleftharpoons S\,(s) + H_2O \quad (1)$$

In the latter case a small oxygen injection to the cooled gas is required, which results to an additional deoxygenation step in the gas cleaning process. A sufficient steam content in gas is also necessary for efficient removal of H_2S on activated carbons [35]. Complete carbonyl sulfide removal by activated carbons is not expected and thus residual COS removal is achieved by hydrolysis to H_2S on metal oxide catalysts at medium temperatures in Guard Bed 1 according to Reaction 2.

$$COS(g) + H_2O(g) \rightleftharpoons H_2S(g) + CO_2(g) \quad (2)$$

While HCN is soluble in water, for full removal a catalytic conversion might be required. HCN hydrolysis at medium temperatures proceeds according to Reaction 3 [36].

$$HCN(g) + H_2O(g) \rightleftharpoons NH_3(g) + CO(g) \quad (3)$$

Simultaneous HCN and COS hydrolysis is possible, as catalysts are very similar in both cases [37]. Due to the versatile nature of activated carbons, organic and inorganic trace impurities, such as BTX compounds, metals, halogens, can be removed in the guard bed steps. The adsorbents employed in the units are primarily non-regenerable.

For CO_2 removal, water scrubbing at elevated pressures is a simpler alternative to organic solvent-based processes, but only feasible for partial CO_2 removal [16]. The investment costs for water-based purification processes are relatively low for a small plant, and its operation and maintenance is simple [38]. Thus, if complete or almost complete CO_2 removal is not required, water scrubbing is a viable low-cost solution.

3. Experimental methods

3.1. Experimental setup

A new PDU-scale final gas cleaning process was constructed for the two week-long tests, Campaign I and II. The process is related in design to the final gas cleaning in the BTL concept and involves all five units

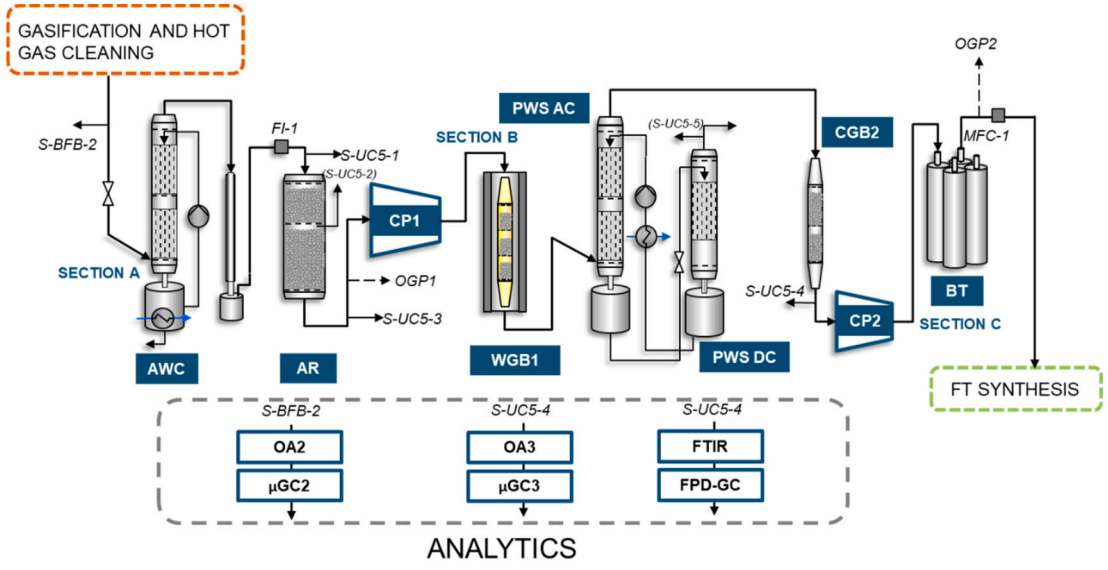

Fig. 2. Schematic of PDU-scale final gas cleaning "UC5", section A (AWC - Acid Wash Column, AR - Adsorbent Reactor, OGP1 - Off-Gas Purge 1, CP1 - Compressor 1), section B (WGB1 - Warm Guard Bed 1, PWS - Pressurized Water Scrubber, AC/DC - Absorption Column/Desorption Column, CGB2 - Cold Guard Bed 2, CP2 - Compressor 2) and section C (BT - Buffer Tank, OGP2 - Off-Gas Purge 2).

listed in Table 2. The purpose of the campaigns was to verify the role of each unit operation in the process train and to assess the suitability of chosen adsorbents and catalysts. An existing gasification test facility, consisting of a bubbling fluidized-bed (BFB) gasifier, a hot gas filter (HF) and a catalytic reformer (CR) was used for syngas generation, and the gasifier was operated in steam/oxygen-blown mode. A mixture of silica sand and dolomite was used as bed material. The filter unit involved two sintered metallic filter elements. The catalytic reformer involved commercial nickel catalysts. The reformer was autothermally operated using a mixture of oxygen and CO_2 as feed gas that was injected on top of the catalyst bed. Three different feedstocks were selected for the test campaigns: bark, forest waste residues (FWR) and straw. The feedstock analyses are given in the Appendix**.** The final gas cleaning process, called "UC5", is schematically represented in Fig. 2.

The final gas cleaning process, UC5, was constructed to match the scale of the synthesis process, with ca. 5 $m^3\ h^{-1}$ (at standard conditions) dry syngas output as design basis. Standard conditions is defined as 101 325 kPa and 273.15 K, and hereafter all flowrates are normalized to standard conditions. In section A (atmospheric pressure) the Acid Wash Condenser (AWC) consisted of a counter-current acid wash column (i.d 0.16 m). The condenser step was followed by an Adsorbent Reactor (AR) involving two-stage fixed bed (i.d 0.25 m). The AR included an air injection, and gas relative humidity (RH) adjustment. The two compressors, CP1 and CP2, were of metal diaphragm type by Sera ComPress GmbH. Section B featured the Warm Guard Bed 1 (WGB1) step which consisted of three-stage fixed bed (i.d 0.08 m), placed in a furnace. The Pressurized Water Scrubber (PWS), which consisted of a pressurized counter-current absorption column (PWS AC) and an atmospheric desorption column (PWS DC) (both i.d 0.16 m) employed N_2 as stripping gas. The final unit in section B was the Cold Guard Bed 2 (CGB2), which was a two-stage fixed bed unit (i.d 0.08 m). A FT synthesis step, not described in Fig. 2, was connected downstream to the final gas cleaning for the entire duration of the campaigns.

Table 3 presents the packed materials. The primary function describes the intended use, however none of the materials are limited to only their primary function.

Four different activated carbon types were utilized in the process, manufactured by Jacobi Carbons. Two of these were non-impregnated virgin carbons, VAC1 and VAC2. Impregnated carbons involved a caustic impregnated carbon, CaAC and acid impregnated carbon AcAC. Literature suggests Al_2O_3 and ZnO having COS hydrolysis promoting effects [39,40] A commercial ZnO adsorbent with alumina, Actisorb S2 by Clariant was therefore used to hydrolyse COS and simultaneously capture the formed H_2S. A Cu/Zn catalyst, CuZn1, Research Catalysts Inc GetterMax® 133, was utilized for the deoxygenation of the syngas.

The bed materials and volumes are presented in detail in the Appendix. Since the final gas cleaning process was first time operated coupled to a FT synthesis process, the UC5 beds were packed to maximum capacity to avoid unwanted breakthrough of impurities. All beds were fresh packed for each campaign. AR was packed with a small top bed of caustic activated carbon, CaAC, followed by a large bed with top layer of VAC1 and bottom layer VAC2. For Campaign II the AR Bed 2 VAC2 packing volume was reduced by 25% from Campaign I. WGB1 two top beds were filled with ZnO1, and the bottom bed was reserved for CuZn1. CGB2 was packed with impregnated carbons.

Table 3
PDU-scale final gas cleaning process UC5 packed materials and volumes for Campaign I and II.

Material	Type	Primary function
VAC1	Non-impregnated AC	Benzene and Tar adsorption
VAC2	Non-impregnated AC	H_2S adsorption
AcAC	H_3PO_4 impregnated acidic AC	NH_3 guard
CaAC	Cu-salt impregnated basic AC	Acid gas guard
ZnO1	ZnO/Alumina adsorbent	COS hydrolysis, H_2S sulfidation
CuZn1	Cu/Zn catalyst	Deoxygenation

3.2. Analytical methods

The analytical instruments were calibrated for small impurities concentrations. The analytical emphasis was in continuous monitoring of gas quality in the cleaned gas for breakthrough of impurities. Small gas quantities are presented as parts per million by volume ($cm^3\ m^{-3}$).

3.2.1. Continuous analytical methods

The gases CO, H_2, CH_4, O_2, N_2 and CO_2 were continuously monitored by ABB manufactured on-line analysers from sampling points after the hot filter S–BFB-1 (OA1), after the reformer S–BFB-2 (OA2) and after UC5 S-UC5-4 (OA3). These were used for real time process monitoring and control. Varian CP-4900 micro gas chromatographs (μGC) with thermal conductivity detectors (TCD) were also utilized and samples were taken from the same points as the OA, and were used in the results calculations for this study. The three micro-GCs (μGC1-3) along with the online analysers were calibrated using a calibration gas mixture in volume fractions of 15% H_2, 15% CO, 15% CO_2, 15% CH_4 and N_2 balance with a relative error of ±2%.

Oxygen breakthrough after final gas cleaning was monitored using the micro gas chromatograph (μGC3) with a specific method for low oxygen concentrations and an estimated limit of detection (LoD) of 0.001 vol % O_2.

For sulfur compound detection, an Agilent 7890A gas chromatograph with a flame photometric detector (FPD-GC) and a GS-GASPRO 30 m × 0.32 mm i.d column with carrier gas He was used. The GC was calibrated using a H_2S and COS containing calibration gas with concentrations 200 $cm^3\ m^{-3}$ and 20.1 $cm^3\ m^{-3}$ respectively, with relative error ±2%. The calibration gas was diluted using N_2 to achieve calibration minimum of 6 $cm^3\ m^{-3}$ H_2S and 0.61 $cm^3\ m^{-3}$ COS. Other sulfur compounds were qualitatively analysed. The LoD for H_2S was estimated at 0.1 $cm^3\ m^{-3}$ and for COS 0.2 $cm^3\ m^{-3}$.

A Fourier transform infrared Spectroscopy (FTIR) of model Gasmet DX4000 was used to measure NH_3, benzene and H_2O content in the cleaned syngas. The component reference ranges were the following: NH_3 20–120 $cm^3\ m^{-3}$, benzene 50–2000 $cm^3\ m^{-3}$and H_2O 0.1–50%. The limits of detection of the compounds were not separately tested in the syngas matrix.

3.2.2. Offline analytical methods

The concentrations of volatile organic compounds from benzene to higher molecular weight components up to pyrene were offline sampled and analysed following the European tar protocol [41]. Tars were sampled in each test setpoint after the hot filtration, S–BFB-1, and after the reformer, S–BFB-1. Nitrogen compounds (NH_3 and HCN) were sampled and analysed after the reformer S–BFB-2. A known gas quantity was injected to a water sample and titrated with HCl for NH_3 determination. For HCN determination the water sample was analysed with a gas chromatograph.

Colorimetric chemical sensor tubes of type Dräger H_2S 2/A (2–200 $cm^3\ m^{-3}$ H_2S, rel. error ±5 to 10%), Dräger H_2S 0.2/a (0.2–5 $cm^3\ m^{-3}$, rel.error ±5 to 10%), Dräger HCN 0.5/a (0.5–5 $cm^3\ m^{-3}$, rel. error 10 to 15%), Dräger SO_2 1/a (1–25 $cm^3\ m^{-3}$, rel. error 10 to 15%) and Dräger HCl 1/a (1–10 $cm^3\ m^{-3}$, rel. error 10 to 15%) were used by the operators for real-time monitoring of the impurities. Some sensor tubes have cross-sensitivities to other impurities in the raw syngas, and therefore this analysis method was primarily employed for the cleaned syngas.

4. Results and discussion

4.1. Syngas generation and composition

The gasification temperature was maintained at around 820 °C with woody biomass feeds, while it was lowered to 710 °C with straw feedstock in order to prevent ash sintering and agglomeration in the gasifier bed. Filtration was conducted in the temperature range of 522–773 °C

Table 4
Setpoint average analysis results after gasification and hot gas cleaning sections.

	Campaign I	Campaign II	
	SP1	SP1	SP2
Feedstock	Bark	FWR	Straw
By volume, dry basis			
CO (%)	22.7	22.5	20.5
H_2 (%)	40.6	40.4	37.4
CO_2 (%)	23.5	20.3	24.2
CH_4 (%)	0.7	0.5	1.8
N_2 (%)	12.5	16.3	16.0
Benzene (g m^{-3})[a]	0.25	0.21	0.41
Water vapour[a]	33.0	29.7	34.8
NH_3 (cm^3 m^{-3})[b]	289	277	710
HCN (cm^3 m^{-3})[b]	1.6	0.8	6.1
H_2S (cm^3 m^{-3})[c]	163	94	314
COS (cm^3 m^{-3})[c]	6.4	5.7	29

[a] Offline tar sampling, S–BFB-2.
[b] Offline N-species sampling, S–BFB-2.
[c] Non-continuous FPD-GC analysis, S-UC5-1.

and the baseline pressure drop across the filter remained stable throughout the test campaigns. The catalytic reformer was operated at maximum ca. 1000 °C and reformer outlet at 900 °C. The well-known poisoning effect of reformer nickel catalysts by H_2S can be largely avoided by operating at 900 °C or above [42,43]. Full conversion of tars and C_2 hydrocarbons was achieved with all the tested feedstocks. Benzene was the only detected residual hydrocarbon in addition to methane. Benzene concentrations measured at reformer outlet were in the range of 0.2–0.4 g m^{-3} corresponding to benzene conversions of 96% with bark and forest residues and 92% with straw. The H_2:CO mol-ratio of the reformed gas was maintained at around 1.8.

Compiled in Table 4 are the main gas analysis results after gasification and the hot gas cleaning section.

4.2. Final gas cleaning

The final gas cleaning process UC5 was operated in upstream coupled mode for a total of 87 h in in each campaign. The longest non-interrupted run was achieved in Campaign I, 43 h. The issues were related to short upstream interruptions in gas feeding. During the downtime the system was N_2 inertized.

The main gas cleaning and process measurement results are summarized in Table 5, in time-weighted average setpoint format, while Fig. 3 illustrates the overall measurement results as a time series. Only values from the specific experimental setpoints were included.

The formic acid:ammonia-ratio gives the consumption of acid in relation to the quantity of gaseous ammonia. The results suggest that in the two measured setpoints the ratio is similar, around 4. FTIR results measured from S-UC5-1 suggest complete or almost complete removal of NH_3 in the AWC step. Ammonia is the main basic syngas impurity that is absorbed at the AWC, and therefore acid is fed in a fixed ratio to keep the circulating water pH constant.

The AR air feeding was maintained fixed at 0.3 dm^3 min^{-1} in both campaigns resulting in fluctuating O_2:H_2S-ratio, with minimimum as low as 1.8. The gas moisture content, expressed as relative humidity (RH), remained between 60 and 80% at the AR.

The exothermic deoxygenation occurring in WGB1 Bed 3 resulted to autothermal operation. The bed temperature was around 10–15 K warmer than the upper ZnO1 beds 1 and 2. The heating of these beds was increased for Campaign II to 205–210 °C from 200 °C in Campaign I.

Table 5
Setpoint average process measurement results for final gas cleaning process UC5.

		Campaign I	Campaign II	
		SP1	SP1	SP2
Temperature (°C)				
AWC	Gas before	153	160	164
	Gas after	21	21	22
AR	Bed 2	33	33	33
WGB1	Bed 1 + 2	200	206	208
	Bed 3	214	216	216
PWS	AC	20	17	17
CGB2	Bed 1 + 2	28	24	23
Other parameters/measurements				
AWC	Water pH	3.01	2.99	2.99
AWC	Formic acid feed rate (cm^3 min^{-1})[a]	0.37	0.35	n.a
AWC	Acid:NH_3 mol ratio	4.0	3.97	n.a
AR	O_2:H_2S mol ratio[b]	3.4	5.9	1.8
AR	RH (%)	78	64	65
PWS	N_2 feed (dm^3 min^{-1})	19	21	22
PWS AC	H_2O flowrate (dm^3 min^{-1})	18.5	18.7	18.6

[a] 100% formic acid.
[b] Based on setpoint average H_2S concentration from Table 4 and measured air feed rate.

The results for the continuous gas analytics and select process measurements, pressure and flowrates, are illustrated as a time series in Fig. 3.

The average pressure level in section A was ca. 4 kPa above atmospheric pressure, and the flowrate in the same section was ca. 110–115 dm^3 min^{-1}. Fig. 3a) and b) top chart area shows the relatively stable gas composition during the gasification setpoints, with only small fluctuations for the major gas components H_2, CO, CO_2 and N_2 (TCD-GC analysed). NH_3 and benzene were not detected in any analysis samples in either campaigns. The bottom chart area in Fig. 3a) and b) shows that a small, but non-continuous, breakthrough of COS occurred. This was evident especially in Campaign 1, where concentrations up to 0.3 cm^3 m^{-3} were detected, especially during the first tens of hours on stream. Breakthrough is believed to be caused by too low WGB1 ZnO1 bed temperature for COS hydrolysis. For Campaign 2 the bed temperatures were increased to above 205 °C, as reported in Table 5, and the breakthrough was consequently almost non-existent. H_2S was not detected in any samples. Other sulfur compounds, such as sulfur oxides and organic sulfurs were qualitatively analysed, and none were detected (within the detection limits of the GC), which is expected since no other sulfur compounds were detected after the hot gas section. Yet it indicates that the oxygen feeding to the cold AR does not cause for example SO_x formation. Fig. 3a) and b) also indicate that pressure fluctuations during the run were minor. As the gas pressure (flow) varies in section A, the majority of the fluctuation is dampened by OGP1, where off-gas flowrate increased or decreases.

The average gas analysis results after the final gas cleaning is given in Table 6. The results are averaged from continuous measurement, using TCD-GC, FTIR and FPD-GC, with the exception of offline colorimetric analysis samples of HCN, HCl and SO_2.

The only confirmed impurity breakthrough was COS, as evident by Fig. 3a) and b). The time weighted average during the course of the campaigns was significantly below 0.1 cm^3 m^{-3}, while highest breakthroughs were up to 0.3 cm^3 m^{-3}. It is noteworthy that the higher COS inlet concentration level in Campaign II SP2 (29 cm^3 m^{-3} versus 5–6 cm^3 m^{-3} in the other setpoints) did not cause a COS breakthrough, suggesting the reaction temperature was adequate also for the higher

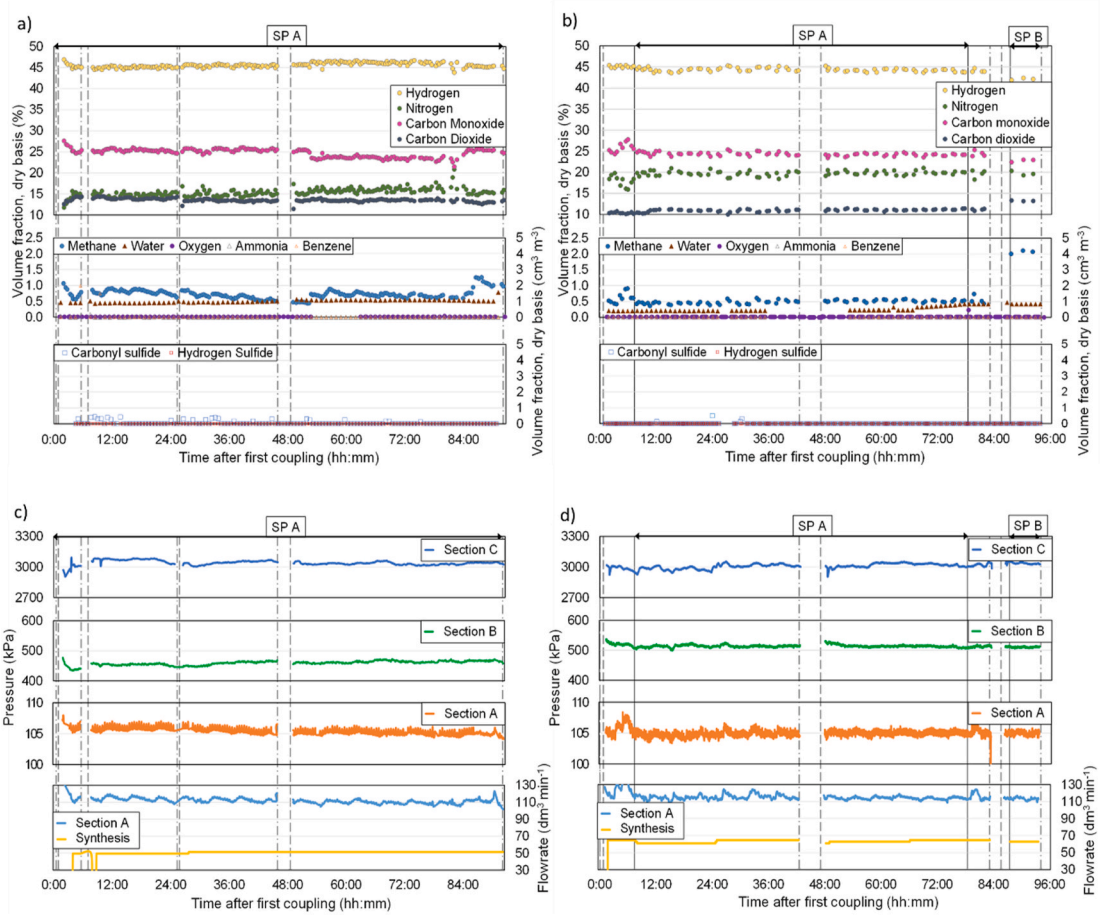

Fig. 3. For a) Campaign I b) Campaign II, continuous gas analysis results after UC5 final gas cleaning from sampling point S-UC5-4. For c) Campaign I d) Campaign II, continuous process measurement results from top chart to bottom chart: section C, B, A pressures and bottom chart for flowrates. Final gas cleaning upstream coupling is indicated with dashed black vertical lines. Setpoint start and stop times indicated with solid black vertical lines. Gas analysis results are indicated with the following markers: dots TCD-GC, triangles FTIR, squares FPD-GC. Colours represent gas components. Solid filled markers utilize left y-axis units and non-filled markers right y-axis units. (For interpretation of the references to color in this figure legend, the reader is referred to the Web version of this article.)

Table 6
Setpoint average gas compositions of cleaned gas, sampled from S-UC5-4.

	Campaign I	Campaign II	
	SP1	SP1	SP2
Average gas composition by volume, dry basis			
CO (%)[a]	24.7	24.4	22.7
H_2 (%)[a]	45.6	44.3	42.2
CO_2 (%)[a]	13.6	11.0	13.3
CH_4 (%)[a]	0.7	0.5	2.0
N2 (%)[a]	15.4	19.8	19.8
O_2 (%)[f]	0/LoD	0/LoD	0/LoD
Benzene (g m^{-3})[b]	0/LoD	0/LoD	0/LoD
NH_3 (cm^3 m^{-3})[b]	0/LoD	0/LoD	0/LoD
Water vapour (%)[c]	0.5	0.2	0.4
H_2S (cm^3 m^{-3})[d]	0/LoD	0/LoD	0/LoD
COS (cm^3 m^{-3})[d]	<0.1	<0.1	<0.1
HCN (cm^3 m^{-3})[e]	0/LoD	0/LoD	0/LoD
HCl (cm^3 m^{-3})[e]	0/LoD	0/LoD	0/LoD
SO_2 (cm^3 m^{-3})[e]	0/LoD	0/LoD	0/LoD

[a] TCD-GC, dry basis.
[b] FTIR, dry basis.
[c] FTIR, wet basis.
[d] FPD-GC, dry basis.
[e] Offline sampling (average) with colorimetric tubes, dry basis.
[f] Measured using a TCD-GC from S-UC5-4 calibrated for low O_2 concentrations. A 0.01% O_2 base level concentration was subtracted from the results.

concentrations. ZnO/alumina acted as a dual functioning COS hydrolysis and H_2S sulfiding adsorbent, similar to what Spies et al. [44] have reported. Almost full COS conversion was achieved by operating the reactor at sufficiently high temperatures.

Ammonia and benzene were not detected at the outlet, thus high removal efficiency in the AWC step was achieved. NH_3 is very water soluble, but it was enhanced by the addition of acid. The full removal of benzene (ca. 60–120 cm^3 m^{-3} in raw syngas) meant that tar compounds were also fully removed. Hydrocarbons are commonly removed by active carbons from gases for example in odour control applications, and can therefore be considered proven technology [45]. Hydrocarbons are primarily reversibly adsorbed and therefore spent activated carbon beds could be regenerated relatively easily. The offline colorimetric analysis samples taken at 1–3 occasions during setpoints indicated that HCN, HCl or SO_2 impurity breakthrough did not occur. Since SO_2 was known not exist in the raw syngas, and HCl concentrations were non-existent or very low (0.2–2 cm^3 m^{-3} from experience of earlier experiments with the same gasification facility). HCN was also totally removed in either the adsorption or water-based scrubbing steps. It was also fully removed in Campaign II SP2 with up to 6 cm^3 m^{-3} inlet concentration.

4.2.1. *Hydrogen sulfide removal*

Manual H_2S measurements during setpoints from various sampling locations after AR Bed 1 (S-UC5-2) and after AR (S-UC5-3), along with the spent adsorbent characterisation were used to gain insights into the stepwise removal of H_2S in the process. Table 7 summarizes these

Table 7
H_2S gas analysis results from multiple sampling locations. Spent adsorbent chracterization: BET-SA and sulfur concentration.

	Fresh	Campaign I	Campaign II	
		SP1	SP1	SP2
Gas H_2S concentration, dry basis ($cm^3\ m^{-3}$)				
After AWC[a]		163	94	314
After AR Bed 1[b]		51	36	246
After AR Bed 2[b]		0	0	0.5
After CGB2[c]		0	0	0
Adsorbent BET-SA ($m^2\ g^{-1}$)[d]				
AR Bed 1 (Surface)	690	639	677	
AR Bed 2 (Surface)	795	617	615	
AR Bed 2 (−15 cm)	950	n.a	860	
AR Bed 2 (−30 cm)	950	n.a	930	
Adsorbent elemental S fraction by mass (%)				
AR Bed 1	0.4[e]	6.7[e]	3.3[f]	
AR Bed 2	0.4[e]	7.4[e]	n.a	

[a] Non-continuous FPD-GC analysis, S-UC5-1.
[b] Colorimetric tube, non-continuous analysis, performed 1–10 h before set-point stop to display maximum breakthrough concentration.
[c] Continuous FPD-GC analysis, S-UC5-4.
[d] Brunauer−Emmett−Teller (BET) surface areas were measured at 77.3 K using a Micrometrics 3Flex analyser using N_2 adsorption isotherms. Samples pre-dried at 150 °C.
[e] Surface sample, CHNS analysis.
[f] Surface sample, Inductively coupled plasma optical emission spectrometry (ICP-OES) analysis.

results.

AR Bed 1 was filled with caustic activated carbon CaAC1. The bed heights were 5 cm and 2.5 cm for Campaign I and Campaign II respectively. The removal rate amounted to over 50% with the low sulfur feedstock setpoints (Campaign I SP1 and Campaign II SP2). This, despite competing adsorption onto the surface by other species, especially benzene. In the high sulfur setpoint (Campaign II, SP2) almost full breakthrough occurred. Köchermann et al. [46] showed that oxygen and steam-free syngas cannot feasibly be desulfurized by activated carbons. Therefore the high removal rate by AR Bed 1 shows that air injection likely promoted H_2S removal. AR Bed 2 contained both VAC1 and VAC2, and H_2S was removed below analysis detection limit (~<0.1 $cm^3\ m^{-3}$) in the low sulfur setpoints. In the high sulfur setpoint a breakthrough of ca. 0.5 $cm^3\ m^{-3}$, was observed and was monitored for 8 h (5 samples) during which the breakthrough did not grow. It suggests that the equilibrium removal rate for the oxidative removal route was reached. The possible reason is that the average O_2:H_2S-ratio was only 1.8, as reported in Table 5, which was not sufficient for complete removal of H_2S.

The post-campaign adsorbent characterisation results show decreased specific surface areas relative to fresh samples. As expected, surface sample available specific surface area and consequently available pore volume decreased most, while the bed samples (−15 cm and −30 cm) showed less decrease. The AR Bed 2 bottom sample BET-SA was 930 $m^2\ g^{-1}$ which is almost equal to fresh sample surface area, suggesting unused bed volume.

Table 8
Setpoint average pressurized water scrubber CO_2 removal rates.

	Campaign I	Campaign II	
	SP1	SP1	SP2
RR_{CO_2} (%)[a]	48	52	53

[a] Removal rate in fractions is calculated as $RR_{CO_2} = \frac{y_{CO_2,OUT} - y_{CO_2,IN}}{y_{CO_2,OUT} - y_{CO_2,OUT} \cdot y_{CO_2,IN}}$ (4) where $y_{CO_2,IN/OUT}$ denotes CO_2 fraction in the PWS AC. IN and OUT gas composition offset by final gas cleaning process estimated average residence time of 10 min.

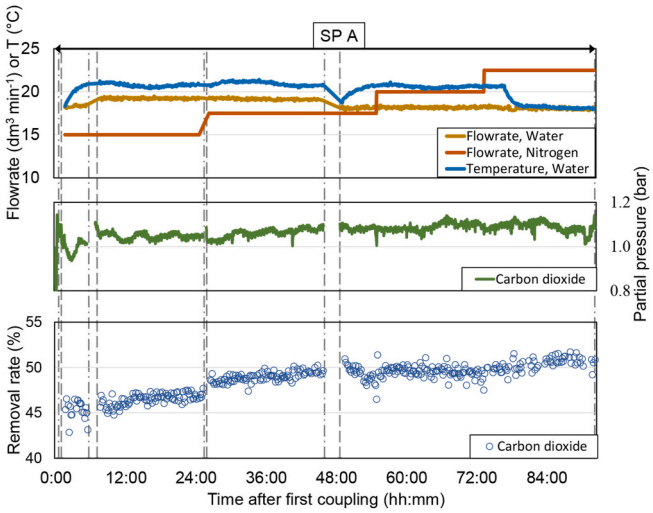

Fig. 4. Campaign I pressurized water scrubber CO_2 removal performance. RR_{CO_2} indicated as blue dots. Green line represents CO_2 partial pressure before PWS (bar), blue line circulating water temperature (°C), orange line PWS DC nitrogen feed ($dm^3\ min^{-1}$), yellow line circulating water flowrate ($dm^3\ min^{-1}$). Final gas cleaning upstream coupling and decoupling is indicated with dashed black vertical lines. (For interpretation of the references to color in this figure legend, the reader is referred to the Web version of this article.)

4.2.2. Pressurized water scrubber

The average CO_2 removal rates calculated using continuous μGC3 data for the two campaigns are presented in Table 8.

Table 8 shows that the Campaign II removal rates are higher than in Campaign I. This is due to higher N_2 feed rate and lower circulating water temperature, and thus up to 53% removal rate was achieved. The liquid-to-gas ratio was kept constant during both campaigns at around 220–250 kg of water per m^3 of syngas at standard conditions.

Fig. 4 visualizes the CO_2 removal as a time series for Campaign I along with operating conditions: CO_2 partial pressure, temperature and flowrates.

Fig. 4 shows that the RR_{CO_2} increased from 46% to almost 52% during the campaign. This was mainly due to manual tuning of PWS conditions in an effort to improve removal. N_2 flow was systematically increased, which directly correlates with the CO_2 removal rate. CO_2 stripping from the gas is thus enhanced by increased N_2 flow as a consequence of improved solubility of CO_2 at the pressure side. The data suggests only marginal benefits of N_2 flowrate above 17.5 $dm^3\ min^{-1}$ (The mol ratio of water to N_2 was ca. 1300). The improved CO_2 removal at the end of the campaign is caused by adjusting the circulation water cooling and the subsequent 2 K drop in water temperature. The results illustrate that the CO_2 removal worked well with no drop in performance, thus showing that no significant contamination of the circulating water occurred during the campaigns.

Table 9
Pressurized water scrubber saturation concentrations c^* of syngas components in water and realized concentrations c from Campaign II SP2 S-UC5-5 stripper gas analysis (PWS DC exit).

	c^* ($\frac{mol}{dm^3}$)	Rel. sol. $\frac{c^*}{c^*_{CO_2}}$	PWS DC exit [a,b] (%)	c ($\frac{mol}{dm^3}$)	*RR* (%)
CO	0.0016	24.6	1.6	0.0012	3.0
H_2	0.0019	20.6	2.6	0.0020	2.7
CO_2	0.0387	1	31.9	0.0243	52.0
N_2	0.0002	47.3	63.7	–	–

[a] By volume, dry basis. Low concentration species, CH_4, was not included.
[b] At the time of measurement, N_2 feed to PWS DC was ca. 20 $dm^3\ min^{-1}$

The PWS DC outlet gas was analysed during Campaign II SP2. To demonstrate the scrubber operational efficiency, the major gas component saturation solubilities in water at Campaign II SP2 PWS AC exit conditions were calculated using Henry's law with experimental parameters obtained from a compilation by Rolf Sander [47]. The results are compiled in Table 9.

From the estimated N_2 volumetric feedrate to the stripper, the PWS component mol balances were calculated to yield removal rates. The removal rate for CO and H_2 was around 3% during the measurement period. The estimated syngas feedrate to PWS DC was 80 $dm^3\ min^{-1}$ and the CO_2 removal rate was 10 $dm^3\ min^{-1}$. If the CO_2 solubility in water had reached saturation, the water circulating rate could have been 36% lower, i.e. 12 $dm^3\ min^{-1}$ or 145 kg water per m^3 syngas. The CO_2 solubility is a bit lower than the saturation prediction when non-idealities of experimental column gas-liquid mass-transfer are factored in.

4.3. Comparison to wet scrubbing technologies

Conventional organic-solvent scrubbing technologies, like Rectisol and Selexol, achieve removal efficiencies proportional to the impurity solubility to the solvent. Removal of H_2S down to <0.1 $cm^3\ m^{-3}$ is possible, thus potentially allowing direct feeding to synthesis, though at the additional cost of a fine wash step. The Rectisol process consists of a prewash step (hydrocarbon removal), main wash (bulk acid gas removal) and often a fine wash step (deep sulfur removal), and utilizes cryogenic methanol [48]. At these extreme conditions CO_2 is mostly removed (95+ %) as well [13]. The Selexol utilizes dimethyl ether/-polyethylene glycol solvent, and is operated at less energy consuming conditions [48]. Thus, the removal limit is higher, likely requiring a further H_2S control step before synthesis. At large scales, the separated acid gas streams are treated by standard sulfur removal technologies such as the Claus process. However, as co-removal of CO_2 is occurring from a syngas stream, sulfur recovery becomes more expensive [13]. For methanol solvent at the Rectisol working conditions, the relative solubility compared to H_2S is higher for NH_3 but lower for COS and HCN [49,50]. For the Selexol, the relative solubility of all the aforementioned compounds is significantly lower than for H_2S, thus requiring additional processing steps for especially COS and HCN. Residual tar removal prior to all acid gas wash processes is required to avoid accumulation to the solvent streams [51]. The final gas cleaning process general technical characteristics are compared to existing wet scrubbing gas cleaning solutions in Table 10.

Both the final gas cleaning process and conventional wet scrubbing processes incur a thermal efficiency penalty for operating at low temperatures and cooling down the syngas, although this heat is partially recoverable. Generally, the wet scrubbing working pressures are higher than used in the process of this study, which in-part operates at atmospheric pressure and medium-pressure range for the PWS. The wet scrubbing processes consume energy for cooling and regenerating the solvent, which contribute to the majority of the operating costs, while majority of the costs of the studied process costs are related to adsorbent replacement, gas compression and PWS water pumping. Adsorption-based cleaning has an advantage at smaller scale or lower impurities concentrations, since the unit operations are simpler and adsorbent replacement quantity small, thus the operating cost is likely more competitive than for the wet scrubbing technologies, which require efficient heat integration regardless of scale. Comparing the cleaning results of the process in this study to alternatives, the achieved purity levels are comparable to the best available wet scrubbing technologies. Summarizing, it can be said that the two technologies are both flexible syngas purification technologies, but they serve different scale and impurity profile purposes with trade-offs that should be weighed case-by-case.

Table 10
Generalized comparison between the final gas cleaning process presented in this study and conventional organic solvent-scrubbing methods [13,48,49].

	This study - Final gas cleaning	Conventional wet scrubbing
Removal method	Adsorption & Absorption (H_2O)	Absorption (solvent)
Temperature	Cold	Cryogenic/Cold
Pressure	Low/medium	Medium/High
Scale	Small/Medium	Large
Gas impurity	Low	Medium/High
Removed impurities	Organic & Inorganic	Organic & Inorganic
Removal level	Parts per billion	Parts per billion/million

5. Conclusions

A simplified deep gas cleaning process, based on adsorbent- and organic solvent-free absorption steps, was successfully piloted and evaluated as an alternative to conventional wet scrubbing technologies for smaller-scale multi-contaminant syngas applications. Gas cleaning performance was assessed in two week-long PDU-scale biomass-to-liquids (BTL) experiments with gasification-generated syngas by an extensive analytical setup for catalyst poison breakthrough. It featured a novel combination of packed bed adsorbents and catalysts for bulk impurities removal mainly facilitated by activated carbons. The system also included a pressurized water scrubber for partial CO_2 removal.

H_2S removal is achieved by the efficient oxidative route on activated carbons with air injection and subsequent deoxygenation. H_2S was completely removed by activated carbons in the first adsorption step (AR). A ZnO-based adsorbent was validated for combined COS hydrolysis and H_2S removal. A small COS breakthrough was detected, which was mitigated by reaction temperature increase. NH_3 was likely completely removed in the first acid wash step, and the low concentration impurity HCN removal was complete. Other minor impurities eg. Benzene and HCl were all were below detection limit after the gas cleaning process. CO_2 removal by water scrubbing achieved a removal rate of 50% with no decrease in performance. The cold guard bed was essentially considered redundant due to the effectiveness of the prior steps. The final gas cleaning process demonstrated the flexible removal of syngas impurities of residual woody- and agricultural-biomass origin. Most notably, the syngas of purity levels suitable for the coupled catalytic Fischer-Tropsch synthesis unit was produced. Hence it was established that the simplified final cleaning concept is sufficient for biomass-derived syngas when combined with the optimized hot gas cleaning process.

Acknowledgements

We acknowledge "COMSYN" project for the financial support. COMSYN has received funding from the European Union's Horizon 2020 research and innovation program under Grant Agreement No. 727476. The work was also financially supported by the "REDIFUEL" project (EU H2020 Grant Agreement No. 817612). The authors would like to thank validation campaign staff, including Ilkka Hiltunen, Teemu Työppönen, Pertti Luoma, Petri Hietula and Aki Braunschweiler, as well as the staff responsible for the analytics.

APPENDIX

Table 1
Properties and composition of gasification feedstock used in Campaign I and II.

Fuel	Campaign I	Campaign II	
	FWR	Bark	Straw
Particle size, (mm)	0.4–1.9	0.4–1.9	
Moisture (%[a])	8.1	8.4	8.1
LHV (MJ kg^{-1})	19.6	19.4	17.3
Volatile matter (%[a])	75.8	77.8	75.5
Ultimate analysis of dry matter (%[a])			
C	52.2	51.5	43.6
H	5.7	5.8	5.6
N	0.5	0.3	0.8
S	0.04	0.06	0.11
O	39.0	38.6	43.6
Cl	n.a	n.a	n.a
Ash	2.6	3.7	6.3

[a]By mass.

Table 2
UC5 packed materials and volumes for Campaign I and II.

Unit	Packing material	Particle size (mm)	Packed volume (dm^3)[a]		$GHSV_{real}$ (h^{-1})[b]	
			Campaign I	Campaign II	Campaign I	Campaign II
AR						
Bed 1	CaAC	4	1.4	1.4	5200	5200
Bed 2	VAC1+VAC2	4	23.4	17.8	300	400
WGB1						
Bed 1 + 2	ZnO1	4.5	2.2	2.2	750	750
Bed 3	CuZn1	2	1.4	1.4	2400	2400
CGB2						
Bed 1	AcAC	1–3	1.1	1.1	1800	1800
Bed 2	CaAC	4	1.1	1.1	1800	1800

[a]Packed volumes estimated from bed masses. The material average densities were based on measured volumes.
[b]Based on estimated flowrates of Section A: 110 dm^3 min^{-1} and Section B: 80 dm^3 min^{-1}. Assumed conditions: AR - 30 °C, 1 bar. WGB1 - 200 °C, 5 bar. CGB2 30 °C, 5 bar.

Declaration of competing interest

The authors declare that they have no known competing financial interests or personal relationships that could have appeared to influence the work reported in this paper.

References

[1] S.S. Ail, S. Dasappa, Biomass to liquid transportation fuel via Fischer Tropsch synthesis - technology review and current scenario, Renew. Sustain. Energy Rev. 58 (2016) 267–286, https://doi.org/10.1016/j.rser.2015.12.143.

[2] M.J.A. Tijmensen, A.P.C. Faaij, C.N. Hamelinck, M.R.M. Van Hardeveld, Exploration of the possibilities for production of Fischer Tropsch liquids and power via biomass gasification, Biomass Bioenergy 23 (2002) 129–152, https://doi.org/10.1016/S0961-9534(02)00037-5.

[3] I. Hannula, E. Kurkela, Liquid Transportation Fuels via Large-Scale Fluidised-Bed Gasification of Lignocellulosic Biomass, 2013. VTT Technology.

[4] T.F. Schulz, L. Barreto, S. Kypreos, S. Stucki, Assessing wood-based synthetic natural gas technologies using the SWISS-MARKAL model, Energy 32 (2007) 1948–1959, https://doi.org/10.1016/j.energy.2007.03.006.

[5] L. Carvalho, E. Furusjö, C. Ma, X. Ji, J. Lundgren, J. Hedlund, M. Grahn, O.G. W. Öhrman, E. Wetterlund, Alkali enhanced biomass gasification with in situ S capture and a novel syngas cleaning. Part 2: techno-economic assessment, Energy 165 (2018) 471–482, https://doi.org/10.1016/j.energy.2018.09.159.

[6] N. Abdoulmoumine, S. Adhikari, A. Kulkarni, S. Chattanathan, A review on biomass gasification syngas cleanup, Appl. Energy 155 (2015) 294–307, https://doi.org/10.1016/j.apenergy.2015.05.095.

[7] A. Molino, V. Larocca, S. Chianese, D. Musmarra, Biofuels production by biomass gasification: a review, Energies 11 (2018) 1–31, https://doi.org/10.3390/en11040811.

[8] E. Kurkela, M. Kurkela, S. Tuomi, C. Frilund, I. Hiltunen, Efficient use of biomass residues for combined production of transport fuels and heat, VTT Technol 347 (2019) 57, https://doi.org/10.32040/2242-122X.2019.T347.

[9] E. Kurkela, M. Kurkela, I. Hiltunen, Steam – oxygen gasification of forest residues and bark followed by hot gas fi ltration and catalytic reforming of tars : results of an extended time test, Fuel Process. Technol. 141 (2016) 148–158, https://doi.org/10.1016/j.fuproc.2015.06.005.

[10] H. Leibold, A. Hornung, H. Seifert, HTHP syngas cleaning concept of two stage biomass gasification for FT synthesis, Powder Technol. 180 (2008) 265–270, https://doi.org/10.1016/j.powtec.2007.05.012.

[11] H. Boerrigter, H. Den Uil, H.-P. Calis, Green diesel from biomass via fischer-tropsch synthesis: new insights in gas cleaning and process design, Pyrolysis Gasif. Biomass Waste, Expert Meet (2002) 1–13.

[12] C.G. Visconti, L. Lietti, P. Forzatti, R. Zennaro, Fischer-Tropsch synthesis on sulphur poisoned Co/Al2O3 catalyst, Appl. Catal. Gen. 330 (2007) 49–56, https://doi.org/10.1016/j.apcata.2007.07.009.

[13] A. de Klerk, Fischer–Tropsch Refining, first ed., Wiley-VCH Verlag GmbH, 2011.

[14] V.S. Sikarwar, M. Zhao, P.S. Fennell, N. Shah, E.J. Anthony, Progress in biofuel production from gasification, Prog. Energy Combust. Sci. 61 (2017) 189–248, https://doi.org/10.1016/j.pecs.2017.04.001.

[15] L. Bailón Allegue, J. Hinge, Biogas and bio-syngas upgrading, DTI Rep (2012) 1–97.

[16] L. Bailón Allegue, J. Hinge, Biogas Upgrading Evaluation of Methods for H 2 S Removal, 2014, pp. 1–31.

[17] P. Mondal, G.S. Dang, M.O. Garg, Syngas production through gasification and cleanup for downstream applications - recent developments, Fuel Process, Technol. 92 (2011) 1395–1410, https://doi.org/10.1016/j.fuproc.2011.03.021.

[18] I. Hannula, Hydrogen enhancement potential of synthetic biofuels manufacture in the European context: a techno-economic assessment, Energy 104 (2016) 199–212, https://doi.org/10.1016/j.energy.2016.03.119.

[19] N. Dahmen, J. Abeln, M. Eberhard, T. Kolb, H. Leibold, J. Sauer, D. Stapf, B. Zimmerlin, The bioliq process for producing synthetic transportation fuels 6, Wiley Interdiscip. Rev. Energy Environ., 2017, https://doi.org/10.1002/wene.236.

[20] H. Thunman, M. Seemann, T. Berdugo Vilches, J. Maric, D. Pallares, H. Ström, G. Berndes, P. Knutsson, A. Larsson, C. Breitholtz, O. Santos, Advanced biofuel production via gasification – lessons learned from 200 man-years of research

activity with Chalmers' research gasifier and the GoBiGas demonstration plant, Energy Sci. Eng. 6 (2018) 6–34, https://doi.org/10.1002/ese3.188.
[21] H. Thunman, C. Gustavsson, A. Larsson, I. Gunnarsson, F. Tengberg, Economic assessment of advanced biofuel production via gasification using cost data from the GoBiGas plant, Energy Sci. Eng. 7 (2019) 217–229, https://doi.org/10.1002/ese3.271.
[22] R. Rauch, H. Hofbauer, A. Chiru, From gasification to synthetic fuels via fischer-tropsch synthesis, Bull. Transilvania Univ. Brasov 3 (2010).
[23] H. Hofbauer, K. Ripfel-nitsche, Report on Gas Cleaning for Synthesis Applications Work Package 2E : " Gas Treatment, 2007.
[24] H. Gruber, P. Groß, R. Rauch, A. Reichhold, R. Zweiler, C. Aichernig, S. Müller, N. Ataimisch, H. Hofbauer, Fischer-Tropsch products from biomass-derived syngas and renewable hydrogen, Biomass Convers. Biorefinery, 2019, https://doi.org/10.1007/s13399-019-00459-5.
[25] S. Tuomi, E. Kurkela, P. Simell, M. Reinikainen, Behaviour of tars on the filter in high temperature filtration of biomass-based gasification gas, Fuel 139 (2015) 220–231, https://doi.org/10.1016/j.fuel.2014.08.051.
[26] M. Husmann, C. Hochenauer, X. Meng, W. De Jong, T. Kienberger, Evaluation of sorbents for high temperature in situ desulfurization of biomass-derived syngas, Energy and Fuels 28 (2014) 2523–2534, https://doi.org/10.1021/ef402254x.
[27] K.P. Yrjas, C.A.P. Zevenhoven, M.M. Hupa, Hydrogen sulfide capture by limestone and dolomite at elevated pressure. 1. Sorbent performance, Ind. Eng. Chem. Res. 35 (1996) 176–183, https://doi.org/10.1021/ie9502749.
[28] W. Mojtahedi, J. Abbasian, H2S removal from coal gas at elevated temperature and pressure in fluidized bed with zinc titanate sorbents. 1. Cyclic tests, Energy & Fuels 9 (1995) 429–434, https://doi.org/10.1021/ef00051a006.
[29] P.J. Woolcock, R.C. Brown, A review of cleaning technologies for biomass-derived syngas, Biomass Bioenergy 52 (2013) 54–84, https://doi.org/10.1016/j.biombioe.2013.02.036.
[30] M.W. Islam, A review of dolomite catalyst for biomass gasification tar removal, Fuel 267 (2020), 117095, https://doi.org/10.1016/j.fuel.2020.117095.
[31] H. Bamdad, K. Hawboldt, S. MacQuarrie, A review on common adsorbents for acid gases removal: focus on biochar, Renew. Sustain. Energy Rev. 81 (2018) 1705–1720, https://doi.org/10.1016/j.rser.2017.05.261.
[32] R.C. Bansal, M. Goyal, Activated Carbon Adsorption, Taylor & Francis, 2005.
[33] F. Sun, J. Liu, H. Chen, Z. Zhang, W. Qiao, D. Long, L. Ling, Nitrogen-rich mesoporous carbons: highly efficient, regenerable metal-free catalysts for low-temperature oxidation of H2S, ACS Catal. 3 (2013) 862–870, https://doi.org/10.1021/cs300791j.
[34] Y. Li, Y. Lin, Z. Xu, B. Wang, T. Zhu, Oxidation mechanisms of H 2 S by oxygen and oxygen-containing functional groups on activated carbon, Fuel Process. Technol. 189 (2019) 110–119, https://doi.org/10.1016/j.fuproc.2019.03.006.
[35] G. Shang, G. Shen, L. Liu, Q. Chen, Z. Xu, Kinetics and mechanisms of hydrogen sulfide adsorption by biochars, Bioresour. Technol. 133 (2013) 495–499, https://doi.org/10.1016/j.biortech.2013.01.114.
[36] O. Kröcher, M. Elsener, Hydrolysis and oxidation of gaseous HCN over heterogeneous catalysts, Appl. Catal. B Environ. 92 (2009) 75–89, https://doi.org/10.1016/j.apcatb.2009.07.021.
[37] D. Chiche, J.M. Schweitzer, Investigation of competitive COS and HCN hydrolysis reactions upon an industrial catalyst: Langmuir-Hinshelwood kinetics modeling, Appl. Catal. B Environ. 205 (2017) 189–200, https://doi.org/10.1016/j.apcatb.2016.12.002.
[38] S. Teir, M. Suomalainen, K. Onarheim, Pre-evaluation of a New Process for Capture of CO 2 Using Water, 2014. https://www.vtt.fi/inf/julkaisut/muut/2014/VTT-R-04035-14.pdf.
[39] Y. Liu, H. He, Experimental and theoretical study of hydrogen thiocarbonate for heterogeneous reaction of carbonyl sulfide on magnesium oxide, J. Phys. Chem. 113 (2009) 3387–3394, https://doi.org/10.1021/jp809887c.
[40] Y. Xu, S. Ju, Z. Wang, Y. Liu, The study of the preparation of catalysts for carbonyl sulfide hydrolysis under moderate temperature, J. Mater. Sci. Chem. Eng. (2018) 31–38, https://doi.org/10.4236/msce.2018.64005, 06.
[41] European Tar Protocol Tc Bt/Tf 143, Biomass Gasification - Tar and Particles in Product Gases -Sampling and Analysis, 2004. http://www.tarweb.net/results/pdf/CEN-Tar-Standard-draft-version-2_1-new-template-version-05-11-04.pdf.
[42] P. Simell, I. Hannula, S. Tuomi, M. Nieminen, E. Kurkela, I. Hiltunen, N. Kaisalo, J. Kihlman, Clean syngas from biomass—process development and concept assessment, Biomass Convers. Biorefinery. (2014) 357–370, https://doi.org/10.1007/s13399-014-0121-y.
[43] M.D. Argyle, C.H. Bartholomew, Heterogeneous catalyst deactivation and regeneration: a review, Catalysts 5 (2015) 145–269, https://doi.org/10.3390/catal5010145.
[44] K.A. Spies, J.E. Rainbolt, X.S. Li, B. Braunberger, L. Li, D.L. King, R.A. Dagle, Warm cleanup of coal-derived syngas: multicontaminant removal process demonstration, Energy and Fuels 31 (2017) 2448–2456, https://doi.org/10.1021/acs.energyfuels.6b02568.
[45] B. Ren, Y. Zhao, N. Lyczko, A. Nzihou, Current Status and Outlook of Odor Removal Technologies in Wastewater Treatment Plant, Waste and Biomass Valorization (2018) 1–16, https://doi.org/10.1007/s12649-018-0384-9.
[46] J. Köchermann, J. Schneider, S. Matthischke, S. Rönsch, Sorptive H2S removal by impregnated activated carbons for the production of SNG, Fuel Process. Technol. 138 (2015) 37–41, https://doi.org/10.1016/j.fuproc.2015.05.004.
[47] R. Sander, Compilation of Henry ' S Law Constants for Inorganic and Organic Species of Potential Importance in Environmental Chemistry, Database, 1999. https://www.ft.unicamp.br/~mariaacm/ST405/Lei de Henry.pdf.
[48] P.M. Maitlis, A. de Klerk, Greener Fischer-Tropsch Processes for Fuels and Feedstocks, 2013, https://doi.org/10.1002/9783527656837.ch16.
[49] R. Sadegh-Vaziri, M. Amovic, R. Ljunggren, K. Engvall, A Medium-scale 50 MWfuel biomass gasification based Bio-SNG plant: a developed gas cleaning process, Energies 8 (2015) 5287–5302, https://doi.org/10.3390/en8065287.
[50] B. Burr, L. Lyddon, A Comparison of Physical Solvents for Acid Gas Removal, 1998. https://bre.com/PDF/A-Comparison-of-Physical-Solvents-for-Acid-Gas-Removal-REVISED.pdf.
[51] L.F. Zubeir, M.H.M. Lacroix, J. Meuldijk, M.C. Kroon, A.A. Kiss, Novel pressure and temperature swing processes for CO2 capture using low viscosity ionic liquids, Separ. Purif. Technol. 204 (2018) 314–327, https://doi.org/10.1016/j.seppur.2018.04.085.